© 2018. Published by The Company of Biologists Ltd | Development (2018) 145, dev166710. doi:10.1242/dev.166710

RESEARCH ARTICLE

Fam46a regulates BMP-dependent pre-placodal ectoderm differentiation in *Xenopus*

Tomoko Watanabe*, Takayoshi Yamamoto, Kohei Tsukano, Sayuki Hirano, Ayumi Horikawa and Tatsuo Michiue‡

ABSTRACT

The pre-placodal ectoderm (PPE) is a specialized ectodermal region which gives rise to the sensory organs and other systems. The PPE is induced from the neural plate border during neurulation, but the molecular mechanism of PPE formation is not fully understood. In this study, we examined the role of a newly identified PPE gene, *Fam46a*, during embryogenesis. *Fam46a* contains a nucleoside triphosphate transferase domain, but its function in early development was previously unclear. We show that *Fam46a* is expressed in the PPE in *Xenopus* embryos, and *Fam46a* knockdown induces abnormalities in the eye formation and the body color. At the neurula stage, *Fam46a* upregulates the expression of PPE genes and inhibits neural crest formation. We also show that Fam46a physically interacts with Smad1/Smad4 and positively regulates BMP signaling. From these results, we conclude that *Fam46a* is required for PPE formation via the positive regulation of BMP signaling. Our study provides a new mechanism of ectodermal patterning via cell-autonomous regulation of BMP signaling in the PPE.

KEY WORDS: Pre-placodal ectoderm, Neural crest, Neural plate border, BMP signaling, *Fam46a*, *Tent5a*, *Xenopus*

INTRODUCTION

Cranial sensory nerve-related organs in the vertebrate are largely differentiated from a specified ectodermal region called the pre-placodal ectoderm (PPE). The PPE is a thick and U-shaped primordium around the neural plate. It is derived from the neural plate border (NPB) at the neurula stage (Couly and Le Douarin, 1985; Baker and Bronner-Fraser, 1997; Holland and Holland, 1999; Baker and Bronner-Fraser, 2001). The PPE differentiates into the anterior pituitary gland and sensory organs, such as the olfactory epithelium, the lens, the trigeminal nerves, the epibranchial nerves, the otic vesicles and the lateral lines (Streit, 2004; Schlosser, 2005, 2006). The neural crest (NC), which is also derived from the NPB, differentiates into sensory nerves and other organs, such as pigment cells, cartilage and secretory cells, mainly in the trunk region (Le Douarin and Kalcheim, 1999; Baker and Bronner-Fraser, 1997; Baker and Bronner-Fraser, 2001). One of the key signaling pathways that organizes the differentiation of PPE and NC cells is the Bone morphogenetic protein (BMP)-mediated pathway.

Department of Life Sciences (Biology), Graduate School of Arts and Sciences, The University of Tokyo, 3-8-1, Komaba, Meguro-ku, Tokyo 153-8902, Japan. *Present address: National Institute of Advanced Industrial Science and Technology, 1-1-1, Higashi, Tsukuba-city, 305-8565 Ibaraki, Japan.

‡Author for correspondence (tmichiue@bio.c.u-tokyo.ac.jp)

T.Y., 0000-0001-8028-6050; K.T., 0000-0003-1905-7376; S.H., 0000-0001-7183-6604; A.H., 0000-0001-9789-4941; T.M., 0000-0001-9047-0513

Received 15 April 2018; Accepted 6 September 2018

BMP is a morphogen that is secreted from the ventral side of the embryo and plays a pivotal role in ectodermal patterning. BMP ligands bind to the receptor, and the intracellular domain of the receptor directly phosphorylates R-Smad (Smad1, Smad5 and Smad8), inducing the formation of their dimer. The R-Smad dimers bind to the signal transducer co-Smad (Smad4) in the cytoplasm, and the complex translocates into the nucleus and binds to the promoter region of the target genes of BMP signaling (Massagué et al., 2005; Kitisin et al., 2007; Schmierer and Hill, 2007). The inhibition of BMP signaling induces the neuroectoderm, whereas the activation of BMP signaling induces the non-neural ectoderm during gastrulation (Weinstein and Hemmati-Brivanlou, 1997; De Robertis and Kuroda, 2004). The NPB is induced between the neuroectoderm and the non-neural ectoderm. It has been reported that NPB differentiation requires at least a transient activation of BMP signaling at gastrula stage (Kwon et al., 2010; Grocott et al., 2012; Saint-Jeannet and Moody, 2014). For PPE and/or NC differentiation from the NPB, moderate or complete inhibition of BMP signaling is considered to be essential after that stage (Brugmann et al., 2004; Glavic et al., 2004; Hong and Saint-Jeannet, 2007; Kwon et al., 2010; Watanabe et al., 2015). The PPE and the NC are thought to complement each other (Leung et al., 2013; Nordin and LaBonne, 2014). However, the differentiation mechanism of these tissues, especially the precise regulation of BMP activity in the PPE, is not fully understood.

To explore novel genes that govern the differentiation of PPE, we previously established a method by which the PPE-like cells were induced from *Xenopus* ectodermal explants, the animal cap, using BMP antagonist Chordin (Chd; Chrd) and Fibroblast growth factor (FGF) inhibitor SU5402 (Watanabe et al., 2015); a weak activation level of FGF signaling is required for PPE induction in addition to an intermediate level of BMP signaling (Ahrens and Schlosser, 2005; Litsiou et al., 2005). Using the PPE-like cells, we performed DNA microarray analysis and successfully identified a novel PPE gene, *Fam46a* (also known as *Tent5a*). *Fam46a* has an NTP transferase-7 domain (Lagali et al., 2002; Kuchta et al., 2009, 2016) and is a causative gene for retinitis pigmentosa and skeletal dysplasia (Diener et al., 2016; Barragán et al., 2008), but its function during early embryogenesis has not been reported. In this study, we examined the role of *Fam46a* for PPE formation. We show that *Fam46a* upregulates PPE specification but inhibits NC formation. Also, *Fam46a* activates BMP signaling by its interaction with Smad1 and Smad4. These results suggest that *Fam46a* defines the PPE region through precise regulation of BMP signaling during early development.

RESULTS

Fam46a is expressed in the PPE, the optic vesicles and the otic vesicles in *Xenopus* embryos

In *Xenopus laevis*, which is an allotetraploid species, the amino acid sequences of two homeologs of *Fam46a* (*Fam46a.L* and *Fam46a.S*)

Development (2018) 145, dev166710. doi:10.1242/dev.166710

were highly similar (Fig. S1A,B). The *Fam46a* gene exists in a broad range of vertebrates, and the amino acid sequences are well conserved among them. In particular, the NTP transferase-7 domain has more than 90% identity with the human and mouse homologs (Fig. S1C,D). The *Fam46* family consists of four paralogs, and they also show a high degree of similarity among them (Fig. S1E,F).

To analyze the change of *Fam46a* expression during embryogenesis, we performed reverse transcription polymerase chain reaction (RT-PCR) analysis and compared *Fam46a* with other ectodermal genes (Fig. 1A). *Fam46a* expression was observed at stage 10 (early gastrula stage). The expression increased further at stage 25 (tailbud stage) and continued to stage 40 (early tadpole stage). *Six1* and *Eya1* (PPE genes) were expressed from stage 12 until stage 40. *Zic1* (an NPB gene), *Vent1* and *Vent2* (BMP target genes) were also expressed from stage 10. These results indicate that *Fam46a* is expressed from approximately the same stage as the expressions of NPB genes and BMP-signaling target genes begin.

Next, we carried out whole-mount *in situ* hybridization from the neurula stage to early tadpole stages (Fig. 1, Fig. S2). At the neurula stage, *Fam46a* was expressed in the PPE region where PPE marker gene *Six1* is expressed (Fig. 1B-C′). At the tailbud stage, *Fam46a* was expressed in the optic vesicles and the otic vesicles (Fig. 1D-D′′). Interestingly, *Fam46a* is not expressed in the lens, which is consistent with the expression pattern of *Six1* and *Eya1* (Pandur and Moody, 2000; David et al., 2001; Ghanbari et al., 2001). At the tadpole stage, *Fam46a* expression was observed in the branchial arch mesenchyme and the retinal pigment epithelium (Fig. 1E,E′). These expression patterns were similar to those of other PPE genes, including *Six1* and *Eya1* (Pandur and Moody, 2000; David et al., 2001). We also examined the subcellular localization of GFP-Fam46a using HeLa cells. At 24 h after transfection, GFP-Fam46a was localized in both the nucleus and the cytoplasm (Fig. 1F). This feature is consistent with that of poly(A) polymerase, one of the NTP transferases (Schmidt and Norbury, 2010).

To further confirm the expression of *Fam46a* in the PPE, we applied the PPE-like cells for quantitative RT-PCR (RT-qPCR) experiments (Watanabe et al., 2015). As expected, *Fam46a* was significantly expressed in the PPE-like cells (*Chd*+SU5402), compared with the uninjected cells, which are known to be an epidermal property (Fig. 2A). Similar to the change of *Fam46a* expression, the PPE genes *Six1* and *Eya1* are highly expressed in the PPE-like cells (Fig. 2B,C), whereas the expression of the epidermal marker gene *XK81* (*Krt12.4*) severely decreased to around one-third (Fig. 2D). In addition, expression of the NP genes *Sox2* and *NCAM* (*Ncam1*) in the PPE-like cells was slightly reduced compared with those injected with only *Chd* (Fig. 2E,F). Expression of the NC genes *FoxD3* and *Snail* (*Snai1*) were not significantly increased in the PPE-like cells (Fig. 2G,H). These results suggest that *Fam46a* is highly expressed in the PPE.

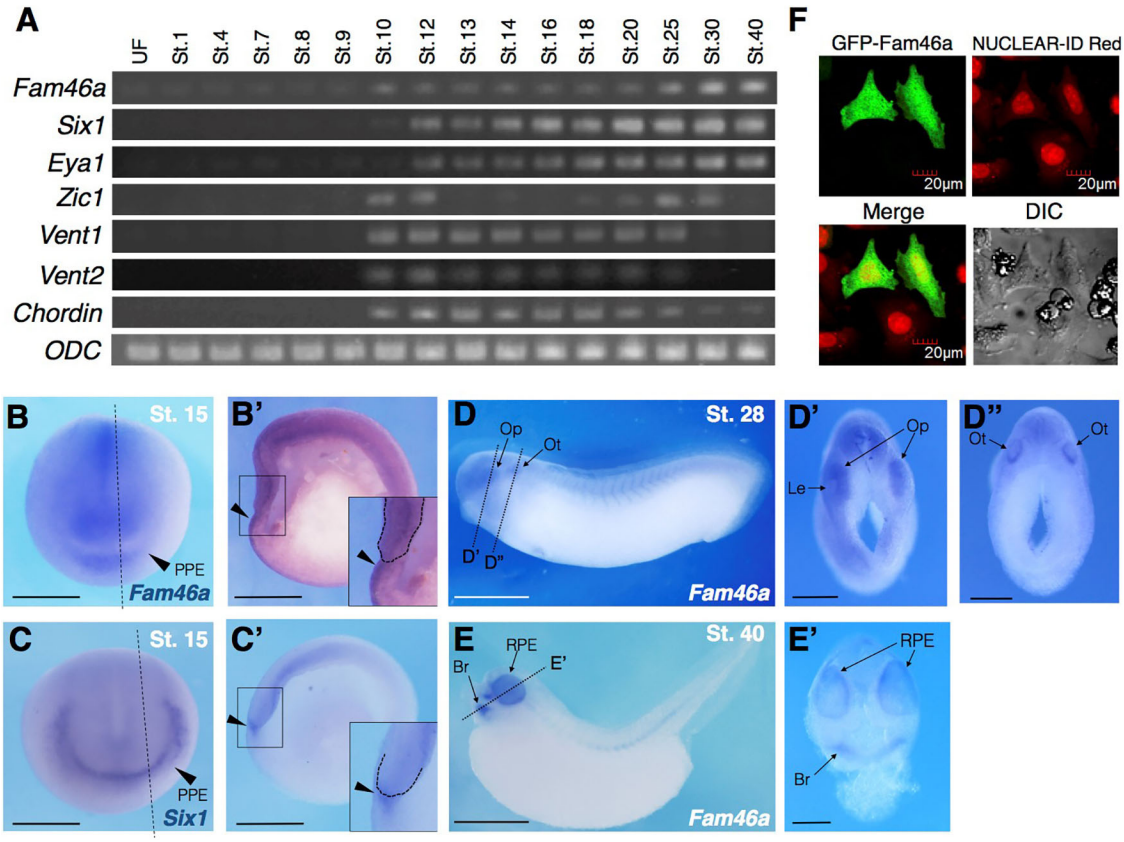

Fig. 1. Temporal and spatial expression pattern of *Fam46a* in *Xenopus*. (A) RT-PCR analysis of *Fam46a* expression. The expression of *Fam46a* is faintly detected from the maternal stage to stage 9, and increased from stage 10, similar to that of *Zic1* (NPB), *Vent1*, *Vent2* (a BMP target gene) and *Chordin* (a BMP antagonist). The expression of two PPE marker genes, *Six1* and *Eya1*, increased soon after the onset of *Fam46a* expression. *ODC* was used as a control. (B-E′) Whole-mount *in situ* hybridization was performed with a *Fam46a* (B,B′,D-D″,E,E′) and *Six1* (C,C′) probe. (B,C) Anterior views; (D,E) lateral views; (B′,C′,D′,D″,E′) hemi-sections. The stage of the embryo is shown in each panel. PPE, pre-placodal ectoderm; Op, optic vesicle; Ot, otic vesicle; Le, lens; Br, branchial arch mesenchyme; RPE, retinal pigment epithelium. (F) HeLa cells were transfected with GFP-Fam46a and cultured for 24 h. Nuclei were stained with NUCLEAR-ID Red. Scale bars: 500 μm in B-C'; 1 mm in D,E; 200 μm in D′,D″,E′; 20 μm in F.

Development (2018) 145, dev166710. doi:10.1242/dev.166710

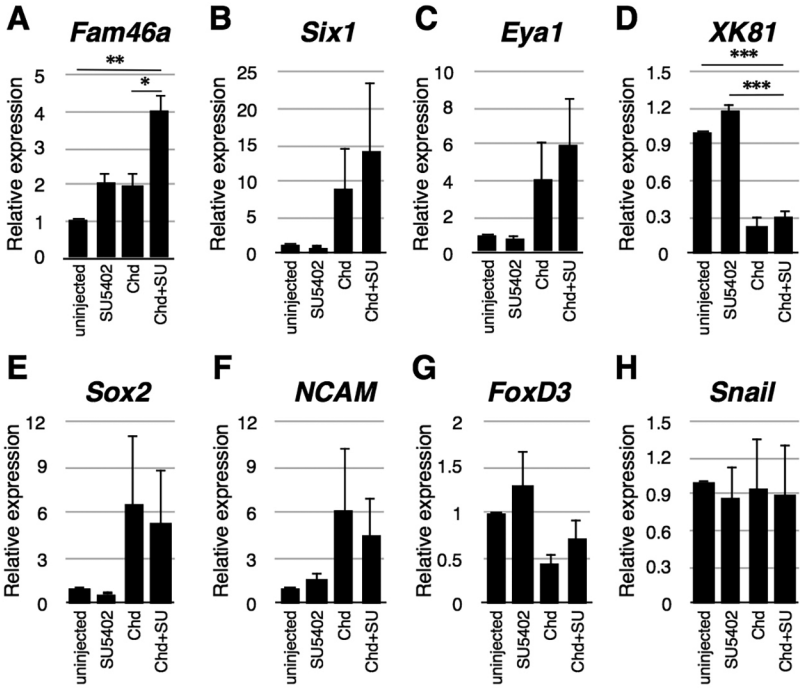

Fig. 2. RT-qPCR analysis of *Fam46a* and other ectodermal marker genes in the PPE-like cells. 20 pg *Chordin* (*Chd*) mRNA was injected into all blastomeres of the four-cell stage embryos. The animal caps were dissected at stage 9 and cultured to stage 15 with or without 25 µM SU5402 (a FGF inhibitor). The expression of *Fam46a*, PPE genes (*Six1* and *Eya1*), an epidermis gene (*XK81*), neural plate genes (*Sox2* and *NCAM*) and NC genes (*FoxD3* and *Snail*) was assessed by RT-qPCR. *EF1α* was used as a control. Unpaired two-tailed *t*-tests were used to determine the statistical significance (**P*<0.05, ***P*< 0.01, ****P*<0.001) (*n*=10, three biological replicates; data are mean±s.e.m.).

Overexpression or knockdown of *Fam46a* induced abnormal body color in *Xenopus* embryos

To analyze the role of *Fam46a* during early development, we overexpressed or knocked down *Fam46a*. Overexpression of *Fam46a* changed the body color to white, decreased the eye area and shortened the body length (Fig. 3A-B′). The eye area was ∼43% (Fig. S3A, S3C) and the body length was ∼86% (Fig. S3B, S3C) of those seen in the normal embryo. The ratio of the white-colored embryos increased in a dose-dependent manner (Fig. 3E). To knockdown *Fam46a*, a morpholino oligo (MO) was designed to inhibit the splicing at the 5′ end of exon 2 in both *Fam46a.L* and *Fam46a.S* genes (Fig. 3F). The *Fam46a* MO was evaluated using RT-PCR. A longer mRNA was observed in *Fam46a* MO-injected embryos (Fig. 3F), indicating that the inhibition of the splicing occurred in *Fam46a*-knockdown embryos, as expected. The *Fam46a* MO-injected embryos appear to be darker than the

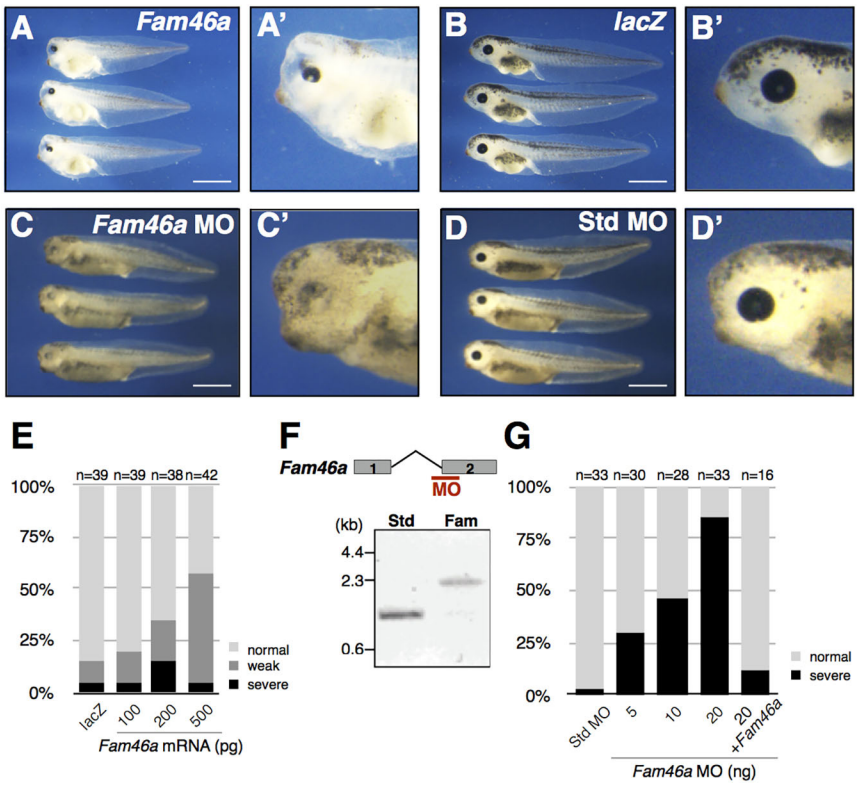

Fig. 3. The phenotypes of gain- and loss-of-function of *Fam46a*. (A-B′) Overexpression of *Fam46a* caused head defects, small eyes and abnormal pigmentation. Lateral views of tadpole embryos injected with 500 pg of *Fam46a* mRNA or *lacZ* mRNA into the animal-dorsal blastomeres at the four-cell stage. (C-D′) Knockdown of *Fam46a* caused retinal defects and abnormal pigmentation. Lateral views of tadpole embryos injected with 20 ng of *Fam46a* MO or standard MO into the animal-dorsal blastomeres at the four-cell stage. (E) The ratio of the phenotypes of *Fam46a* mRNA-injected embryos are summarized as bar graphs. Severe phenotypes include absence of eyes, head expansion and abnormal pigmentation. Weak phenotype refers to the embryos that show only abnormal pigmentation. (F) The design of *Fam46a* MO. (Top) The binding position of *Fam46a* MO (red). Gray boxes indicate the exons (with the exon number) and the black line indicates the intron, the length of which is 1.3 kb. This MO was designed to block the splicing of both *Fam46a.L* and *Fam46a.S*. The lower image shows the result of RT-PCR using standard MO (Std)- or *Fam46a* MO (Fam)-injected embryos. (G) The ratio of the phenotypes of *Fam46a* MO-injected embryos is summarized as bar graphs. The embryos that showed retinal defects and abnormal pigmentation were classified into 'severe phenotype'. The specificity of MO effects was confirmed by rescue experiments, in which *Fam46a* MO was co-injected with *Fam46a* mRNA. Scale bars: 1 mm.

Development (2018) 145, dev166710. doi:10.1242/dev.166710

standard MO-injected embryo, and the retina area was grossly reduced at the early tadpole stage (Fig. 3C-D′), whereas the body length was not obviously altered. The ratio of individuals exhibiting the retinal disorder phenotypes increased in a dose-dependent manner (Fig. 3G). To further confirm the specificity of the MO, *Fam46a* MO and *Fam46a* mRNA were co-injected, and the number of abnormal tadpoles decreased (Fig. 3G). This result indicates that the phenotypes we observed were dependent on the inhibition of *Fam46a*. As pigment cells are known to be derived from the NC region cells, the body color phenotype in *Fam46a*-modulated embryos suggests that *Fam46a* plays a role not only in PPE but also in NC formation.

Fam46a induces PPE formation, but inhibits NC specification

To further examine the role of *Fam46a* in PPE and NC specification, we next analyzed the expression pattern of ectodermal marker genes in embryos injected with mRNA or MO of *Fam46a*. When *Fam46a* mRNA was injected, the area of expression of *Six1*, a PPE gene, was expanded (Fig. 4A, upper), whereas *Fam46a* MO injection caused the reduction of the *Six1*-expressed region (Fig. 4A, lower). *Fam46a* overexpression reduced the expressions of *Slug* (*Snai2*) and *FoxD3* (NC marker genes), whereas *Fam46a* knockdown induced a remarkable expansion of NC genes' expression (Fig. 4B). Interestingly, when *Fam46a* MO was injected, the NC gene expression region expanded into the area where the expression of the PPE gene was reduced. We also examined the expression pattern of other ectodermal genes. *Fam46a* overexpression slightly reduced the expression of *XK81* and *Sox3* (a neural plate marker gene) (Fig. 4C, upper), whereas *Fam46a* knockdown slightly increased the expression of these genes (Fig. 4C, lower). It should be noted that the overexpression or knockdown of *Fam46a* did not show the described phenotype at a high frequency. This may be because mRNA or MO is generally spread to a limited area in *Xenopus* embryos. From these results, we conclude that *Fam46a* induces PPE formation, but inhibits specification of the NC, epidermis and neural plate (Fig. 4D).

At the late neurula stage, the PPE region subdivides into the anterior, the lateral and the posterior PPE (Schlosser, 2006; Saint-Jeannet and Moody, 2014). We next examined the expression of *Six3* (an anterior PPE gene), *Ath-3* (Neurod4; a lateral PPE gene) and *Pax8* (a posterior PPE gene). *Fam46a* knockdown reduced the expression of these genes (Fig. S4A), but expanded that of a posterior NPB gene (*Pax3*), an eye-marker gene (*Pax6*) and a cement gland gene (*Muc2*) (Fig. S4B). These results suggest that *Fam46a* is necessary for each placode formation and other ectodermal region specification.

To confirm the role of *Fam46a* in PPE and NC specification, we applied the PPE-like cells and the NC-like cells

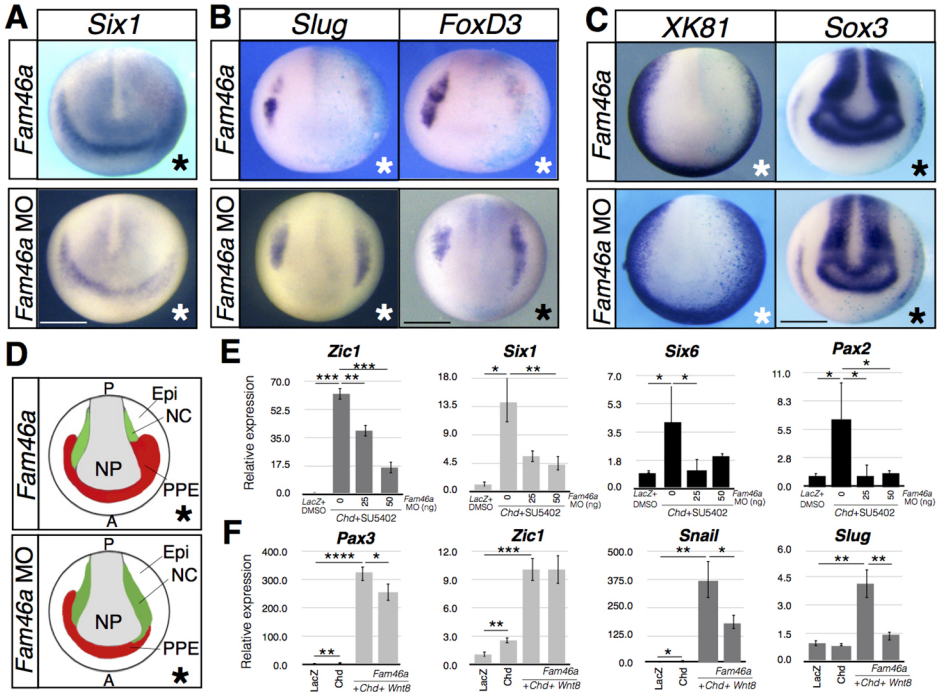

Fig. 4. *Fam46a* is required for the PPE but inhibits the NC specification. (A-C) Whole-mount *in situ* hybridization analysis of *Six1* (PPE), *Slug* (NC), *FoxD3* (NC), *XK81* (epidermis) and *Sox3* (neural plate) expression patterns in *Xenopus* embryos injected with *Fam46a* mRNA or *Fam46a* MO [with a tracer (*lacZ*)]. Embryos were injected at the four-cell stage and collected at the early neurula stage (stage 15). The asterisk denotes the injected side, which was labeled by staining β-galactosidase (β-gal). The sample sizes are as follows: *Six1* (*Fam46a* *n*=58/102, *Fam46a* MO *n*=81/131), *Slug* (*Fam46a* *n*=25/60, *Fam46a* MO *n*=21/55), *FoxD3* (*Fam46a* *n*=24/59, *Fam46a* MO *n*=21/37), *XK81* (*Fam46a* *n*=9/9, *Fam46a* MO *n*=9/24) and *Sox3* (*Fam46a* *n*=7/22, *Fam46a* MO *n*=10/18). (D) Schematic figures of the ectodermal pattern in *Fam46a* mRNA or *Fam46a* MO-injected embryos, referred to as in A-C. The asterisks indicate the injected side. A, anterior; P, posterior; red, PPE; green, NC; gray, neural plate (NP); white, epidermis. (E) Embryos at the four-cell stage were injected in their animal side with *Chordin* (*Chd*) and *Fam46a* MOs. The animal caps were dissected at the blastula stage and were cultured until early neurula stage (stage 15) with or without SU5402. The expression level of *Zic1* (NPB), *Six1* (PPE), *Six6* (anterior PPE) and *Pax2* (posterior PPE) were then analyzed by RT-qPCR (*n*=20, three biological replicates, error bars represent s.e.m.). Each value was normalized to the level of *EF1α* expression. (F) *Chd*, *Wnt8* and *Fam46a* mRNA were injected into the animal side of the four-cell stage embryos. The animal caps were dissected at the blastula stage and the specimens were cultured as in E. The expression levels of NPB genes (*Pax3* and *Zic1*) and NC genes (*Snail* and *Slug*) were then analyzed by RT-qPCR (*n*=20, three biological replicates, error bars represent s.e.m.). Each value was normalized to the level of *EF1α* expression. Unpaired two-tailed *t*-tests were used to determine the statistical significance (*P<0.05, **P<0.01, ***P<0.001, ****P<0.0001). Scale bars: 500 µm.

Development (2018) 145, dev166710. doi:10.1242/dev.166710

(Watanabe et al., 2015) and analyzed the expression of ectodermal genes. In the PPE-like cells, *Zic1* (an NPB gene), *Six1* (a PPE gene), *Six6* (an anterior PPE gene) and *Pax2* (a posterior PPE gene) were expressed (Fig. 4E and Fig. S5A). However, the expression was severely reduced by the knockdown of *Fam46a*. In the NC-like cells, NPB genes (*Pax3* and *Zic1*) and NC genes (*Snail* and *Slug*) were expressed (Fig. 4F and Fig. S5B). When *Fam46a* mRNA was injected, the expression of *Pax3*, *Snail* and *Slug* was reduced, but there was no effect on the expression of *Zic1* (Fig. 4F and Fig. S5B). These results confirm that *Fam46a* upregulates the expression of both NPB and PPE genes, whereas it strongly inhibits NC marker gene expression, consistent with our *in vivo* analyses. In addition, considering the role of *Zic1* in PPE formation (Jaurena et al., 2015), *Fam46a* possibly regulates PPE formation through the maintenance of *Zic1*.

Fam46a regulates PPE formation via the modulation of BMP signaling

To further investigate how Fam46a regulates PPE specification, we analyzed an intracellular signaling pathway, BMP signaling. BMP signaling plays a major role in ectodermal patterning, and it has also been shown that Fam46a is one of the Smad1-associating proteins in humans (Colland et al., 2004). These reports suggest that Fam46a regulates PPE formation by modulating BMP signaling with Smad1. To examine this, we applied the type II receptor of BMP (BMPRII; also known as bmpr2) and a truncated type I BMP receptor (tBR) (Suzuki et al., 1994). As already reported, the overexpression of *BMPRII* induces the expression of the BMP target genes *Vent1* and *Vent2*, whereas the expression of *tBR* reduces these expressions (Fig. 5A). Similar to the overexpression of *BMPRII*, the overexpression of *Fam46a* increased the expression of *Vent1* and *Vent2*, but the knockdown did not (Fig. 5B). These results indicate that *Fam46a* enhances the expression of BMP target genes. To confirm these results, we also performed RT-qPCR using the animal cap. When *Fam46a* was overexpressed, the expression of both *Vent1* and *Vent2* was increased (Fig. 5C).

The low expression of *tBR* is known to expand the expression of *Six1*, *FoxD3* and *Sox2*, and to inhibit that of *XK81* (Fig. 5D and E, upper) (Sato et al., 2005). Interestingly, when *Fam46a* mRNA was co-injected with the low dose of *tBR*, the expression region of *Six1* was drastically expanded (Fig. 5D and E, lower). However, *Sox2* expression was not significantly reduced, probably because *Sox2* is weakly expressed in the PPE. The expression of *FoxD3* and *XK81* was almost lost, or reduced. It is possible that *Fam46a* no longer rescues *XK81* expression because *tBR* greatly reduces BMP signaling. These results suggest that *Fam46a* plays an important role in PPE differentiation by adjusting the level of BMP signaling.

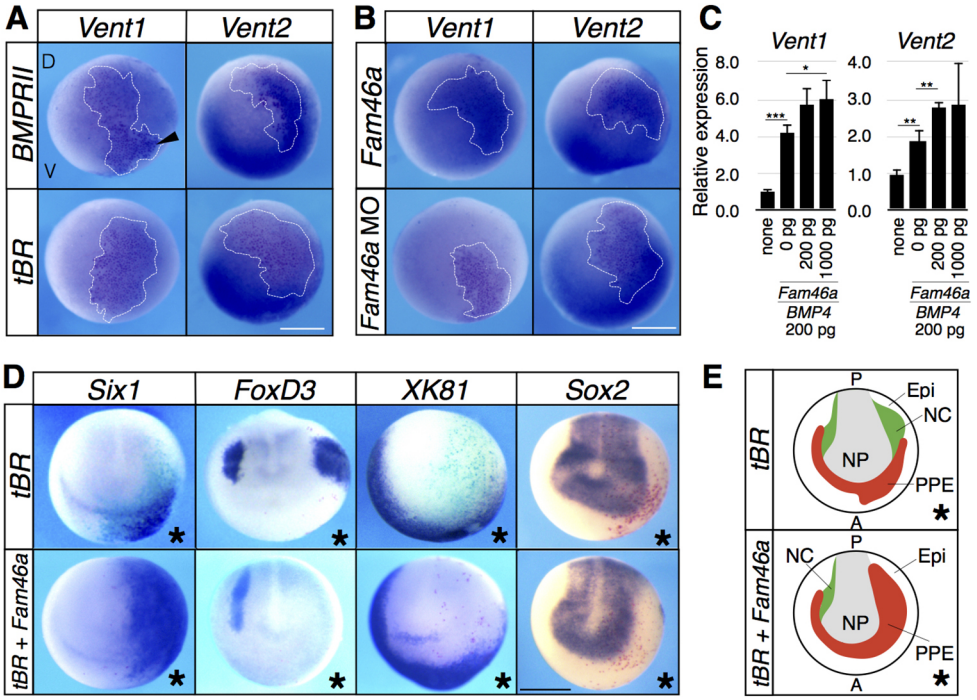

Fig. 5. *Fam46a* regulates PPE specification by modulating BMP signaling. (A,B) The expression of *Vent1* and *Vent2* at blastula stage. Embryos were injected with 500 pg of *BMPRII* mRNA, *tBR* mRNA, *Fam46a* mRNA or 5 ng of *Fam46a* MO [with a tracer (*lacZ*)] at the four-cell stage. The specimens were collected at stage 10.25. Outlines indicate the injected cells, colored with red-gal. All images are orientated in the animal-pole view (the upper side is the dorsal side, and vice versa). Arrowhead indicates the ectopic expression of *Vent1* in BMPRII-expressed embryos. Endogenous expression of *Vent2* was also observed in the ventral region (U-shape). Sample sizes were as follows: *Vent1* (*BMPRII* n=8/9, *tBR* n=11/11, *Fam46a* n=14/16, *Fam46a* MO n=19/19) and *Vent2* (*BMPRII* n=17/19, *tBR* n=12/13, *Fam46a* n=13/17, *Fam46a* MO n=16/16). (C) RT-qPCR analysis of BMP-signal activity using the animal cap that was injected with *BMP4* and *Fam46a* mRNA. The explants were collected at the early neurula stage (stage 15) and analyzed by RT-qPCR (n=20, three biological replicates, error bars represent s.e.m.). Each value was normalized to the level of *EF1α* expression. Unpaired two-tailed *t*-tests were used to determine statistical significance (*P<0.05, **P<0.01, ***P<0.001). (D) Whole-mount *in situ* hybridization experiments examining *Six1*, *FoxD3*, *XK81* and *Sox2* expression patterns in the embryos injected with 250 pg of *tBR* mRNA or 250 pg *tBR* mRNA + 250 pg *of Fam46a* mRNA. Embryos were injected at the four-cell stage and were collected at the early neurula stage (stage 15). An asterisk indicates the injected side with staining for β-galactosidase (β-gal) as the lineage tracer. Sample sizes were as follows: *Six1* (*tBR* n=8/10, *tBR*+*Fam46a* n=6/10), *FoxD3* (*tBR* n=5/11, *tBR*+*Fam46a* n=10/12), *XK81* (*tBR* n=10/10, *tBR* +*Fam46a* n=10/10) and *Sox2* (*tBR* n=9/9, *tBR*+*Fam46a* n=8/9). (E) Ectoderm pattern diagram in *tBR* mRNA or *tBR* mRNA+ *Fam46a* mRNA-injected embryos (refers to D). Asterisk indicates the injected side. NP, neural plate. Scale bars: 500 µm.

Development (2018) 145, dev166710. doi:10.1242/dev.166710

To investigate how Fam46a is involved in BMP signaling, we next examined the change of Fam46a localization in response to BMP addition. We transfected GFP-Fam46a into HeLa cells and observed the fluorescent signal before and after the addition of BMP4. GFP-Fam46a started to accumulate in the nucleus, from the cytoplasm, after BMP4 addition, and this distinct nuclear localization was still present after 60 min (Fig. S6A-C). These results indicate that Fam46a protein translocates into the nucleus in response to BMP signal activation.

Fam46a physically interacts with Smad1 and Smad4

We next examined the direct interaction between Fam46a and BMP signaling components by immunoprecipitation experiments. Western blot analysis indicated that Fam46a physically binds to Smad1 (Fig. 6A). The signal intensity of the precipitates of Smad1 indicates that the binding of Fam46a-Smad1 was weaker than that of Smad1-Smad4 (Fig. 6B). To examine whether Fam46a and Smad1 bind to each other when BMP signaling is not activated, we conducted the same experiment in the presence of LDN193189, an inhibitor of the BMPR type I receptor. The binding of Fam46a and Smad1 was observed even under the inhibition of BMP signaling (Fig. 6C). Next, to identify the binding domain of Smad1 with Fam46a, we performed immunoprecipitation experiments using the deletion constructs of Smad1 (Fig. 6D). Smad1 has two domains: the MH1 domain has a DNA-binding motif, and the MH2 domain includes a SSXS motif, which is phosphorylated by BMPRII. The two domains are separated by a linker sequence. Using the three types of constructs, we found that Fam46a binds to full-length Smad1 (Smad1-WT) and Smad1-MH1, but not to Smad1-MH2. This indicates that Fam46a interacts with MH1 and/or a linker domain of Smad1. Fam46a appeared to interact with Smad1-MH1 more strongly than with Smad1-WT (Fig. 6E). We also examined the interaction between Fam46a and Smad4. There was a strong interaction between Fam46a and Smad4, similar to the binding between Smad2 and Smad4 (Fig. 6F,G).

Because the subcellular localization of Smad1 is known to be important for BMP signaling, we next examined the localization of mCherry-Smad1 under Fam46a-expressed conditions. Canonical Wnt signaling is known to induce organizer-triggering invagination. Therefore, to maintain BMP signaling in the blastula ectoderm, we used *β-catenin* (*ctnnb1*) MO for the inhibition of invagination (Inomata et al., 2013). In *β-catenin* MO and *mCherry-Smad1* mRNA-injected embryos, the mCherry-Smad1 nuclear localization level was high (Fig. S7A, 1st line). In *Chd* mRNA-injected embryos, the ratio of mCherry-Smad1 localization in the nucleus decreased (Fig. S7A, 2nd line). When *Chd* and *Fam46a* mRNA were co-injected, mCherry-Smad1 was localized again in the nucleus (Fig. S7A, 3rd line). The nucleus-to-cytoplasm ratio of Smad1 localization was quantitatively evaluated using ImageJ (Fig. S7B). From these results, we concluded that Fam46a promotes the nuclear localization of Smad1.

Fam46a activates BMP signaling via the stabilization of Smad1

Our data showed that Fam46a physically interacts with Smad1 and Smad4 and promotes BMP target gene expression. We further investigated the mechanisms of transcriptional regulation of BMP

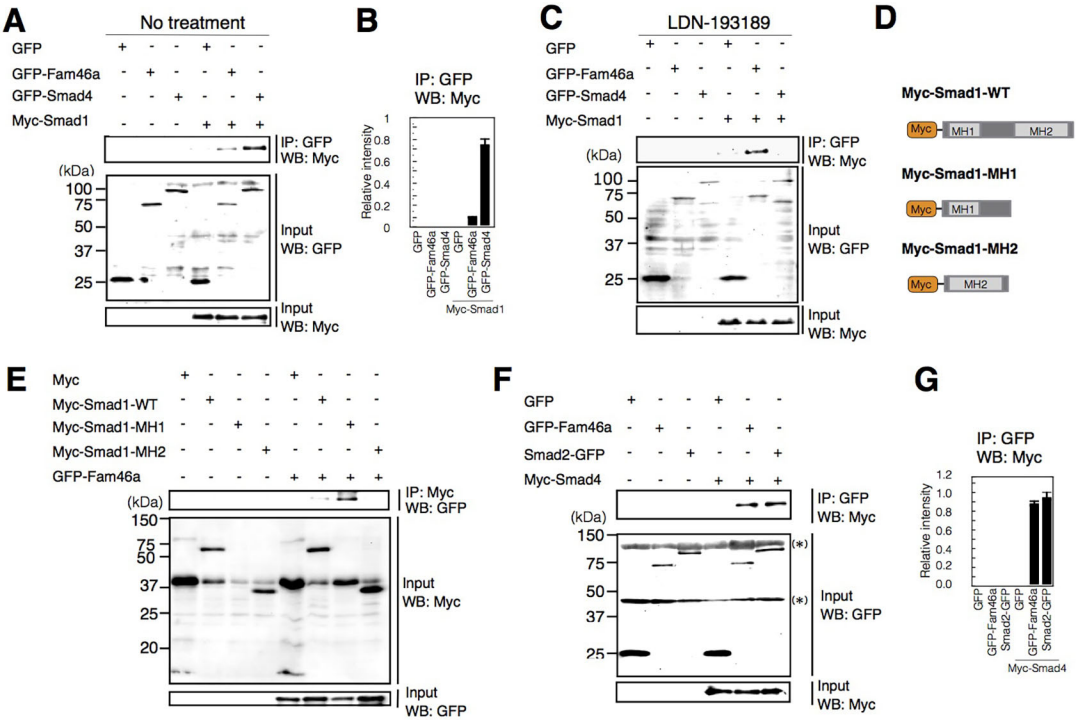

Fig. 6. Fam46a interacts with Smad1 and Smad4 in *Xenopus* embryos. (A,C) Immunoprecipitation assays were performed using the lysates of the embryos injected with *GFP*, *GFP-Fam46a* or *GFP-Smad4*, and *Myc-Smad1* mRNA, which had been cultured until the early gastrula stage (stage 10.5) (n=10) with or without 100 nM LDN-193189. (B) Quantitative analysis of the precipitates of GFP or GFP-tagged proteins in A using ImageJ (three biological replicates, error bars represent s.e.m.). Each value was normalized to the level of each input protein. (D) Schematic figure of the construct of Myc-Smad1-WT, Myc-Smad1-MH1 and Myc-Smad1-MH2. (E) An immunoprecipitation assay using the embryos injected with *Myc*, *Myc-Smad1-WT*, *Myc-Smad1-MH1*, *Myc-Smad1-MH2* and *GFP-Fam46a* mRNA, and cultured until early gastrula stage (stage 10.5) (n=10). (F) An immunoprecipitation assay using the embryos injected with *GFP*, *GFP-Fam46a*, *Smad2-GFP* and *Myc-Smad4* mRNA, and cultured until stage 10.5 (n=10). The asterisks indicate nonspecific bands. (G) Quantitative analysis of the precipitates of GFP or GFP-tagged proteins in F using ImageJ (three biological replicates, error bars represent s.e.m.). Each value was normalized to the level of each input protein.

Development (2018) 145, dev166710. doi:10.1242/dev.166710

target genes by Fam46a. In this experiment, we used a *Vent2-TCFm-Luc* reporter construct containing a *Vent2* promoter, which has mutations in the TCF-binding site and only consists of BMP responsive elements (Hikasa et al., 2010). The *Vent2-TCFm-Luc* reporter was stimulated by *BMP4* expression, and also by *Fam46a* expression (Fig. 7A). However, co-expression of *BMP4* and *Fam46a* did not enhance the luminescence intensity (Fig. 7A). This result suggests that *BMP4* or *Fam46a* expression caused the strong activation and no stronger activation was seen by co-expression. On the other hand, when *Fam46a* was knocked down, *Vent2-TCFm-Luc* reporter activation was severely reduced, even in the presence of BMP4 (Fig. 7B). These results indicate that *Fam46a* is required for the activation of BMP target gene transcription via a *Vent2* reporter.

As we described above, we found that Fam46a interacts with MH1/linker domain of Smad1 (Fig. 6E). Smad1 protein is known to be constantly degraded in the cytosol through its phosphorylation on the linker region by Glycogen synthase kinase 3 (GSK-3β) or Mitogen-activated protein kinase (MAPK) (Wnt/FGF signaling components), followed by polyubiquitylation (Fuentealba et al., 2007; Ueberham and Arendt, 2013). So, we examined the amount of Smad proteins present when Fam46a was expressed, to evaluate whether Fam46a is involved in this process. In *Myc-Smad1* mRNA-injected embryos, we observed two Smad1 forms, the phosphorylated form and the unphosphorylated form (Fig. 7C). When *GFP-Fam46a* was expressed, the amount of phosphorylated Smad1 was not significantly altered, whereas the amount of unphosphorylated Smad1 increased (Fig. 7C,E). We also examined the amount of Smad4 protein in *Fam46a*-expressing cells. When *GFP-Fam46a* was expressed, the amount of Smad4 remained unaltered (Fig. 7D). Together, these results suggest that Fam46a also facilitates BMP signaling via the stabilization of Smad1, not Smad4.

DISCUSSION

The new PPE-related gene *Fam46a*

In this study, we identify a novel PPE gene, *Fam46a*, and reveal the crucial role of *Fam46a* in PPE formation. This provides a new regulatory mechanism of BMP-signal activity with an intracellular factor in the PPE.

BMP signaling is required for PPE induction at the early gastrula stage, but the level of the signaling after that stage is still controversial: complete inhibition at late gastrula stage (Ahrens and Schlosser, 2005; Litsiou et al., 2005; Kwon et al., 2010) or intermediate level at early neurula stage (Brugmann et al., 2004; Glavic et al., 2004; Hong and Saint-Jeannet, 2007; Watanabe et al., 2015). Our study shows that Fam46a overexpression induces PPE formation through BMP-signal activation. This suggests that the complete inhibition of BMP signaling is not necessarily required for PPE induction.

PPE and NC arise from the common precursor NPB at late gastrula stage. To distinguish the PPE from the NC, the proper level of FGF signaling is required for PPE formation, while the proper level of Wnt signaling is necessary for NC formation (Sato et al., 2005; Groves and LaBonne, 2014; Saint-Jeannet and Moody, 2014). In addition to these differences, *Sox5*, which acts as an inhibitor of BMP signaling, upregulates NC specification and inhibits PPE formation through the modulation of BMP signaling

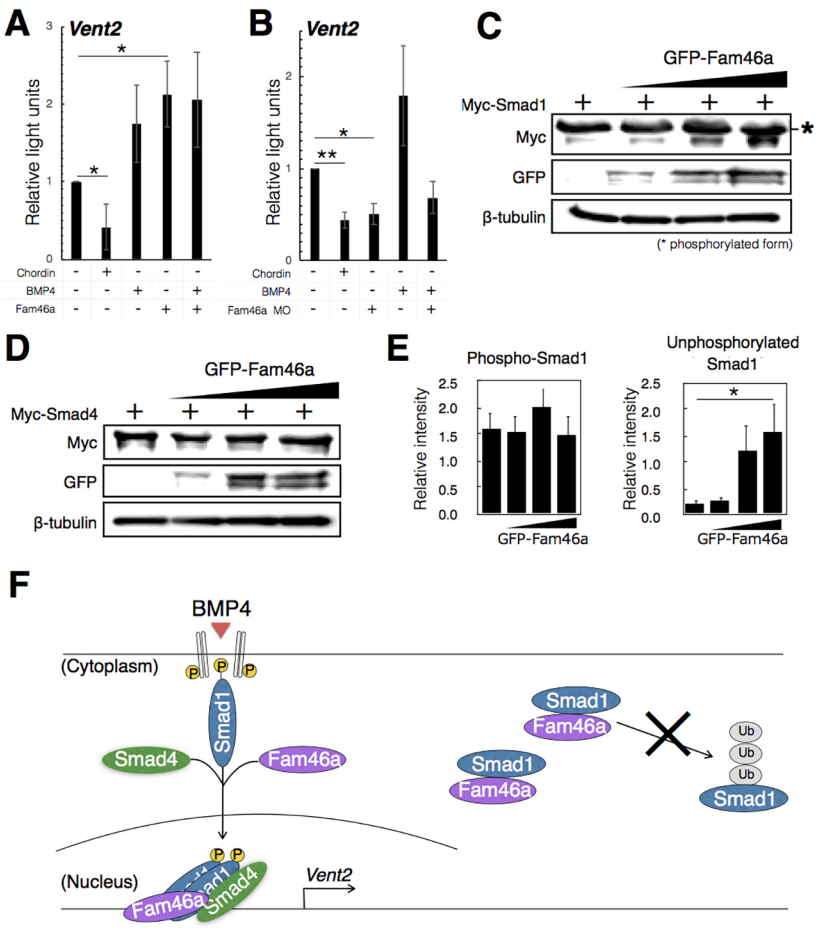

Fig. 7. *Fam46a* regulates Smad1 stabilization. (A,B) Luciferase assay using the *Vent2-TCFm-Luc* reporter construct in the presence of *Chordin*, *BMP4*, *Fam46a* or *Fam46a* MO. Embryos were injected at the four-cell stage and were incubated to early gastrula stage (stage 10.5) (n=10, three biological replicates, error bars represent s.e.m.). Unpaired two-tailed t-tests were used to determine statistical significance (*P<0.05, **P<0.01). (C,D) Western blot analysis using embryos injected with *Myc-Smad1*(C) or *Myc-Smad4* (D) and *GFP-Fam46a* (C,D) at the four-cell stage and cultured until early gastrula stage (stage 10.5) to examine the amount of Myc-Smad1 or Myc-Smad4 (n=10 each). β-Tubulin was used as a control. The asterisks indicate phosphorylated Smad. (E) Quantification of phosphorylated and unphosphorylated Smad1 in C. Each value was normalized to the level of β-tubulin expression (three biological replicates, error bars represent s.e.m.). Unpaired two-tailed t-tests were used to determine statistical significance (*P<0.05). (F) A schematic model of BMP signaling regulated by Fam46a.

Development (2018) 145, dev166710. doi:10.1242/dev.166710

(Nordin and LaBonne, 2014). Our study also reveals that *Fam46a* activates BMP signaling and induces the formation of PPE, not that of NC. These studies suggest that, in addition to the different requirement on FGF and Wnt signaling, BMP activity is slightly different between the PPE and the NC. Thus, the discrete activities of BMP signaling are possibly important for the selective differentiation of the PPE and the NC. The difference in the intracellular components, including Fam46a, could make clear boundary of the signaling activity, which is not easily accomplished by the gradient of growth factors.

The molecular function of Fam46a in BMP signaling activation

It has been shown that human Fam46a is associated with Smad1 by the yeast two-hybrid analysis (Colland et al., 2004), but how Fam46a is involved in BMP signaling has not been clarified. Our study shows that Fam46a binds to both Smad1 and Smad4 and activates the transcription of BMP target genes (Fig. 7). We also found that *Fam46a* enhances the stabilization of Smad1 protein, but does not increase the amount of the phosphorylated protein (Fig. 7C,E). Smad1 protein is known to be constantly degraded in the cytosol through phosphorylation in its linker region by GSK-3β or MAPK (Wnt/FGF signaling components), followed by polyubiquitylation (Fuentealba et al., 2007; Ueberham and Arendt, 2013). It is possible that the binding of Fam46a with Smad1-MH1 and linker region in the cytosol causes the inhibition of Smad1 phosphorylation and subsequent degradation, and that the stabilization of Smad1 promotes the activation of BMP signaling.

It has been reported that human Fam46a interacts with Bag6 (previously known as Bat3) (Etokebe et al., 2015). This protein interacts with Smad1 and negatively regulates BMP signaling (Goto et al., 2011). It is also possible that Fam46a competes with Bag6 for association with Smad1, thereby enhancing BMP signaling.

In addition, based on analyses of the amino acid sequence and three-dimensional structure, Fam46a was recently reported as one of the non-canonical poly(A) polymerases (Kuchta et al., 2016; Mroczek et al., 2017). Non-canonical poly(A) polymerases add a poly(A) tail to pre-mRNA 3′-UTR ends after transcription (Richter, 1999). Because of this, this enzyme is considered to increase the stability of mRNA (Richter, 1999). These analyses suggest that it is also possible that Fam46a contributes to the stabilization of Smad mRNAs. Further analysis is required to reveal whether mRNAs are stabilized by Fam46a.

In summary, we have represented two possible modes of Fam46a function in BMP signaling in a schematic (Fig. 7F). In the first mode, when the BMP ligand associates with the receptor, Fam46a binds to both Smad1 and Smad4, and this complex translocates into the nucleus. This complex then binds to the promoter of a BMP target gene and activates transcription. In the second mode, Fam46a is involved in Smad1 stabilization and indirectly activates the BMP signaling pathway. Smad1 is constantly marked by ubiquitylation and is degraded, but Fam46a inhibits this process. In conclusion, Fam46a regulates PPE specification via the activation of BMP signaling in this region. In addition, the efficiency of PPE induction in mammalian stem cells is lower than in other ectodermal tissues. Because the amino acid sequences of *Fam46a* in *Xenopus* and human are highly similar, the finding of the role of *Fam46a* in PPE formation in *Xenopus* will contribute not only to developmental biology, but also to the stem cell field.

MATERIALS AND METHODS

Xenopus embryo manipulation

All experiments using *Xenopus laevis* were approved by The Office for Life Science Research Ethics and Safety, University of Tokyo. Frogs (wild type; female, 90 g-119 g; male, >60 g) were purchased from Watanabe Zoshoku (Hyogo, Japan). The developmental stages of *Xenopus* embryos were determined according to the standard description (Nieuwkoop and Faber, 1994). Fertilized eggs were obtained by artificial fertilization, and the embryos were de-jellied by 4.6% L-cysteine hydrochloride in 1×Steinberg's solution (SS) (pH 7.8). Embryos were cultured in 1×SS to stage 9 and then placed in 0.1×SS to the appropriate stage.

Microinjection

Xenopus Fam46a was cloned into a vector: pCS2 or pCS2-GFP. In this study, pCS2-*Chordin* (*Chd*), pCS2-*Wnt8*, pCS2-*BMP4*, pCS2-GFP, pCS2-GFP-*Fam46a*, pCS2-GFP-*Smad4*, pCS2-6-Myc-*Smad1*, pCS2-*Smad2*-GFP, pCS2-6-Myc-*Smad4*, pCS2-6-Myc-MH1-*Smad1* and pCS2-6-Myc-MH2-*Smad1* were used as templates for *in vitro* transcription. mRNAs were transcribed *in vitro* using the mMESSAGE mMACHINE SP6 Kit (Invitrogen) and were then microinjected with a picoinjector PLI-100 (Harvard Apparatus) in 5% Ficoll/1×SS. Injected embryos were cultured to stage 9 and were then placed into 0.1×SS.

MO experiments

The morpholino antisense oligonucleotides (MOs) that we used in this study were designed as follows:

Fam46a-MO, 5′-GCCTCCTGCAATGTGAAATATAAGA-3′;

Standard control oligo (Std-MO), 5′-CCTCTTACCTCAGTTACAATTTATA-3′.

Fam46a-MO was synthesized against two *Xenopus* homoeologous genes, *Fam46a.L* and *Fam46a.S*, to block the exon-intron splicing (Fig. 3F). The sequence of the Std-MO was referred to Gene Tools.

Whole-mount *in situ* hybridization

In situ hybridization was performed as described previously (Morita et al., 2013). For lineage tracing, *lacZ* mRNA-injected embryos were stained with Red-Gal (Sigma-Aldrich) or X-Gal (Wako). The digoxigenin (DIG)-labeled RNA probes for *Fam46a*, *Six1*, *Eya1*, *Slug*, *FoxD3*, *Snail*, *XK81*, *Sox3* and *Sox2* were transcribed *in vitro*. The signals with a DIG-labeled RNA probe were detected with NBT-BCIP (Roche).

Animal cap assay

The animal cap is the animal pole region of *Xenopus* blastula. The cells were manually dissected at stage 8.5-9 with forceps and tungsten needles, and the specimens were cultured in 1×SS until stage 15.

RT-PCR

Total RNA was purified by ISOGEN II (Nippon Gene). Reverse transcription was carried out using SuperScript III Reverse Transcriptase (Invitrogen). PCR was performed with ExTaq DNA polymerase (TakaraBio). RT-qPCR was performed using the KAPA SYBR FAST qPCR Kit (KAPA Biosystems). Primer sets used for PCR are listed in Table S1.

Results shown are representative of at least three biological replicates. Error bar represents S.E. between the triplicate sets. Unpaired two-tailed *t*-tests were used to determine the statistical significance.

Cell culture

HeLa cells were cultured in Dulbecco's Modified Eagle's Medium (High Glucose) (Wako) containing 10% fetal bovine serum (Cell Culture Bioscience) and 1% Penicillin-Streptomycin (Sigma-Aldrich) under 5% CO_2 at 37°C. Transfections were performed using Lipofectamine 3000 transfection kit (Invitrogen) according to the manufacturer's instructions. Transfected cells were cultured in the medium for 24 h, then treated with or without BMP4 (100 ng/ml). The nuclei were stained by NUCLEAR-ID Red (Enzo), according to the manufacturer's instructions.

Development (2018) 145, dev166710. doi:10.1242/dev.166710

Confocal imaging

HeLa cell images were acquired with a confocal microscope (Olympus) using UPLSAPO 20×objective. After taking pre-images, cells were treated with or without BMP4 (100 ng/ml) and then cultured for 120 min in 37°C, 5% CO_2. Images were captured at the time points of 0 min, 60 min and 120 min after BMP4 treatment.

Quantitative analysis of Fam46a nuclear translocation

The GFP-Fam46a fluorescence intensities in the cytoplasm and nuclear were quantified using ImageJ. The nuclear/cytoplasm ratios were calculated for each cell and compared between pre- and 120 min-images.

Western blot analysis

Embryos were lysed in RIPA buffer [0.1% NP40, 20 mM Tris-HCl (pH 8), 10% glycerol] supplemented with a protease inhibitor cocktail (Roche). Proteins were detected using the following antibodies: anti-Myc (1:1000, 562, Medical and Biological Laboratories), anti-GFP (1:1000, GTX113617, GeneTex), anti-β-tubulin (1:1000, ab6046, Abcam), anti-pSMAD1 (1:6000, #06-702, EMD Millipore) and anti-SMAD1 (1:1000, #9512, Cell Signaling Technology). Secondary antibodies that were conjugated with horseradish peroxidase were applied and detected by chemiluminescence using Chemi-Lumi One L (Nacalai Tesque).

Immunoprecipitation

Immunoprecipitation experiments were performed according to the manufacturer's instructions (GE Healthcare Life Science). Briefly, embryos were lysed with Lysis buffer [1% NP-40, 20 mM Tris-HCl (pH 8.0), 137 mM NaCl, 10% glycerol, 2 mM EDTA] supplemented with protease inhibitor cocktail (Roche). The supernatant was incubated with anti-GFP (1:100, sc-9996, Santa Cruz Biotechnology) or anti-Myc (1:100, 562, Medical and Biological Laboratories) for 1 h at 4°C, then incubated with protein G sepharose (GE Healthcare) for 24 h at 4°C, and analyzed by immunoblotting.

Luciferase assay

Luciferase reporter DNA, *Renilla* luciferase DNA and the indicated mRNA or MO were co-injected into both cells of two-cell embryos. Embryos were cultured to stage 10.5, three sets of ten embryos were collected and assayed with a Dual-Luciferase Reporter Assay System (Promega) and Fluoroskan Ascent FL plate reader (Thermo Fisher Scientific). Error represents S.E. between the triplicate sets. Unpaired two-tailed *t*-tests were used to determine the statistical significance.

Acknowledgements

We thank Drs Y. Ito, Y. Onuma, S. Matsukawa and K. Mizuno for technical advice. We also thank Drs H. Hikasa and S. Sokol for critical discussion and for providing the *Vent2-TCFm-Luc* reporter construct.

Competing interests

The authors declare no competing or financial interests.

Author contributions

Conceptualization: T.M.; Methodology: T.W., T.M.; Formal analysis: T.W.; Investigation: T.W., T.Y., K.T., S.H., A.H., T.M.; Data curation: T.W., T.Y., K.T., S.H., A.H.; Writing - original draft: T.W., T.Y., T.M.; Writing - review & editing: T.W., T.Y., K.T., S.H., A.H., T.M.; Supervision: T.Y., T.M.; Project administration: T.M.; Funding acquisition: T.M.

Funding

Our study was supported in part by a Japan Society for the Promotion of Science KAKENHI (22570200) to T.M.

Supplementary information

Supplementary information available online at
http://dev.biologists.org/lookup/doi/10.1242/dev.166710.supplemental

Reference

Ahrens, K. and Schlosser, G. (2005). Tissues and signals involved in the induction of placodal *Six1* expression in *Xenopus laevis*. *Dev. Biol.* **288**, 40-59.

Baker, C. V. H. and Bronner-Fraser, M. (1997). The origins of the neural crest. Part I: embryonic induction. *Mech. Dev.* **69**, 3-11.

Baker, C. V. H. and Bronner-Fraser, M. (2001). Vertebrate cranial placodes I. Embryonic induction. *Dev. Biol.* **232**, 1-61.

Barragán, I., Borrego, S., Abd El-Aziz, M. M., El-Ashry, M. F., Abu-Safieh, L., Bhattacharya, S. S. and Antiñolo, G. (2008). Genetic analysis of FAM46A in Spanish families with autosomal recessive retinitis pigmentosa: characterisation of novel VNTRs. *Ann. Hum. Genet.* **72**, 26-34.

Brugmann, S. A., Pandur, P. D., Kenyon, K. L., Pignoni, F. and Moody, S. A. (2004). *Six1* promotes a placodal fate within the lateral neurogenic ectoderm by functioning as both a transcriptional activator and repressor. *Development* **131**, 5871-5881.

Colland, F., Jacq, X., Trouplin, V., Mougin, C., Groizeleau, C., Hamburger, A., Meil, A., Wojcik, J., Legrain, P. and Gauthier, J. M. (2004). Functional proteomics mapping of a human signaling pathway. *Genome Res.* **14**, 1324-1332.

Couly, G. F. and Le Douarin, N. M. (1985). Mapping of the early neural primordium in quail-chick chimeras. I. Developmental relationships between placodes, facial ectoderm, and prosencephalon. *Dev. Biol.* **110**, 422-439.

David, R., Ahrens, K., Wedlich, D. and Schlosser, G. (2001). *Xenopus Eya1 d*emarcates all neurogenic placodes as well as migrating hypaxial muscle precursors. *Mech. Dev.* **103**, 189-192.

De Robertis, E. M. and Kuroda, H. (2004). Dorsal-ventral patterning and neural induction in *Xenopus* embryos. *Annu. Rev. Cell. Dev. Biol.* **20**, 285-308.

Diener, S., Bayer, S., Sabrautzki, S., Wieland, T., Mentrup, B., Przemeck, G. KH., Rathkolb, B., Graf, E., Hans, W., Fuchs, H. et al. (2016). Exome sequencing identifies a nonsense mutation in Fam46a associated with bone abnormalities in a new mouse model for skeletal dysplasia. *Mamm. Genome* **27**, 111-121.

Etokebe, G. E., Zienolddiny, S., Kupanovac, Z., Enersen, M., Balen, S., Flego, V., Bulat-Kardum, L., Radojčić-Badovinac, A., Skaug, V., Bakke, P. et al. (2015). Association of the FAM46A gene VNTRs and BAG6 rs3117582 SNP with non small cell lung cancer (NSCLC) in Croatian and Norwegian populations. *PLoS ONE* **10**, e0122651.

Fuentealba, L. C., Eivers, E., Ikeda, A., Hurtado, C., Kuroda, H., Pera, E. M. and De Robertis, E. M. (2007). Integrating patterning signals: Wnt/GSK3 regulates the duration of the BMP/SMAD1 signal. *Cell* **131**, 980-993.

Ghanbari, H., Seo, H.-C., Fjose, A. and Brändli, A. W. (2001). Molecular cloning and embryonic expression of *Xenopus* Six homeobox genes. *Mech. Dev.* **101**, 271-277.

Glavic, A., Maris Honoré, S., Gloria Feijóo, C., Bastidas, F., Allende, M. L. and Mayor, R. (2004). Role of BMP signaling and the homeoprotein Iroquois in the specification of the cranial placodal field. *Dev. Biol.* **272**, 89-103.

Goto, K., Tong, K. I., Ikura, J. and Okada, H. (2011). HLA-B-associated transcript 3 (Bat3/Scythe) negatively regulates SMAD phosphorylation in BMP signaling. *Cell Death Dis.* **2**, e236.

Grocott, T., Tambalo, M. and Streit, A. (2012). The peripheral sensory nervous system in the vertebrate head: a gene regulatory perspective. *Dev. Biol.* **370**, 3-23.

Groves, A. K. and LaBonne, C. (2014). Setting appropriate boundaries: fate, patterning and competence at the neural plate border. *Dev. Biol.* **389**, 2-12.

Hikasa, H., Ezan, J., Itoh, K., Li, X., Klymkowsky, M. W. and Sokol, S. Y. (2010). Regulation of TCF3 by Wntdependent phosphorylation during vertebrate axisspecification. *Dev. Cell* **19**, 521-532.

Holland, L. Z. and Holland, N. D. (1999). Chordate origins of the vertebrate central nervous system. *Curr. Opin. Neurobiol.* **9**, 596-602.

Hong, C.-S. and Saint-Jeannet, J.-P. (2007). The activity of *Pax3* and *Zic1* regulates three distinct cell fates at the neural plate border. *Mol. Biol. Cell* **18**, 2192-2202.

Inomata, H., Shibata, T., Haraguchi, T. and Sasai, Y. (2013). Scaling of dorsal-ventral patterning by embryo size-dependent degradation of Spemann's organizer signals. *Cell* **153**, 1296-1311.

Jaurena, M. B., Juraver-Geslin, H., Devotta, A. and Saint-Jeannet, J.-P. (2015). Zic1 controls placode progenitor formation non-cell autonomously by regulating retinoic acid production and transport. *Nat. Commun.* **6**, 7476.

Kitisin, K., Saha, T., Blake, T., Golestaneh, N., Deng, M., Kim, C., Tang, Y., Shetty, K., Mishra, B. and Mishra, L. (2007). Tgf-Beta signaling in development. *Sci. STKE.* **399**, cm1.

Kuchta, K., Knizewski, L., Wyrwicz, L. S., Rychlewski, L. and Ginalski, K. (2009). Comprehensive classification of nucleotidyltransferase fold proteins: identification of novel families and their representatives in human. *Nucleic Acids Res.* **37**, 7701-7714.

Kuchta, K., Muszewska, A., Knizewski, L., Steczkiewicz, K., Wyrwicz, L. S., Pawlowski, K., Rychlewski, L. and Ginalski, K. (2016). FAM46 proteins are novel eukaryotic non-canonical poly(A) polymerases. *Nucleic Acids Res.* **44**, 3534-3548.

Kwon, H.-J., Bhat, N., Sweet, E. M., Cornell, R. A. and Riley, B. B. (2010). Identification of early requirements for preplacodal ectoderm and sensory organ development. *PLoS Genet.* **6**, e1001133.

Lagali, P. S., Kakuk, L. E., Griesinger, I. B., Wong, P. W. and Ayyagari, R. (2002). Identification and characterization of *C6orf37*, a novel candidate human retinal disease gene on chromosome 6q14. *Biochem. Biophys. Res. Commun.* **293**, 356-365.

Le Douarin, N. M. and Kalcheim, C. (1999). *The Neural Crest.* Cambridge University Press.

Leung, A. W., Kent Morest, D. and Li, J. YH. (2013). Differential BMP signaling controls the formation and the differentiation of multipotent preplacodal ectoderm progenitors from human embryonic stem cells. *Dev. Biol.* **379**, 208-220.
Litsiou, A., Hanson, S. and Streit, A. (2005). A balance of FGF, BMP and WNT signalling positions the future placode territory in the head. *Development* **132**, 4051-4062.
Massagué, J., Seoane, J. and Wotton, D. (2005). SMAD transcription factors. *Genes Dev.* **19**, 2783-2810.
Morita, M., Yamashita, S., Matsukawa, S., Haramoto, Y., Takahashi, S., Asashima, M. and Michiue, T. (2013). Xnr3 affects brain patterning via cell migration in the neural-epidermal tissue boundary during early Xenopus embryogenesis. *Int. J. Dev. Biol.* **57**, 779-786.
Mroczek, S., Chlebowska, J., Kuliński, T. M., Gewartowska, O., Gruchota, J., Cysewski, D., Liudkovska, V., Borsuk, E., Nowis, D. and Dziembowski, A. (2017). The non-canonical poly(A) polymerase FAM46C acts as an onco-suppressor in multiple myeloma. *Nat. Commun.* **8**, 619.
Nieuwkoop, P. D. and Faber, J. (1994). *Normal Table of Xenopus Laevis (daudin)*. New York: Garland Sciences.
Nordin, K. and LaBonne, C. (2014). *Sox5* Is a DNA-binding cofactor for BMP R-SMADs that directs target specificity during patterning of the early ectoderm. *Dev. Cell.* **31**, 374-382.
Pandur, P. D. and Moody, S. A. (2000). *Xenopus Six1* gene is expressed in neurogenic cranial placodes and maintained in the differentiating lateral lines. *Mech. Dev.* **96**, 253-257.
Richter, J. D. (1999). Cytoplasmic polyadenylation in development and beyond. *Microbiol. Mol. Biol. Rev.* **63**, 446-456.
Saint-Jeannet, J.-P. and Moody, S. A. (2014). Establishing the pre-placodal region and breaking it into placodes with distinct identities. *Dev. Biol.* **389**, 13-27.
Sato, T., Sasai, N. and Sasai, Y. (2005). Neural crest determination by co-activation of *Pax3* and *Zic1* genes in *Xenopus* ectoderm. *Development* **132**, 2355-2363.
Schlosser, G. (2005). Evolutionary origins of vertebrate placodes: Insights from developmental studies and from comparisons with other deuterostomes. *J. Exp. Zool. B. Mol. Dev. Evol.* **304**, 347-399.
Schlosser, G. (2006). Induction and specification of cranial placodes. *Dev. Biol.* **294**, 303-351.
Schmidt, M. J. and Norbury, C. J. (2010). Polyadenylation and beyond: emerging roles for noncanonical poly(A) polymerases. *Wiley Interdiscip Rev. RNA.* **1**, 142-151.
Schmierer, B. and Hill, C. S. (2007). TGFbeta-SMAD signal transduction: molecular specificity and functional flexibility. *Nat. Rev. Mol. Cell. Biol.* **8**, 970-982.
Streit, A. (2004). Early development of the cranial sensory nervous system: from a common field to individual placodes. *Dev. Biol.* **276**, 1-15.
Suzuki, A., Thies, R. S., Yamaji, N., Song, J. J., Wozney, J. M., Murakami, K. and Ueno, N. (1994). A truncated bone morphogenetic protein receptor affects dorsal-ventral patterning in the early *Xenopus* embryo. *Proc. Natl. Acad. Sci. USA* **91**, 10255-10259.
Ueberham, U. and Arendt, T. (2013). The Role of SMAD Proteins for Development, Differentiation and Dedifferentiation of Neurons, Trends in Cell Signaling Pathways in Neuronal Fate Decision, Dr Sabine Wislet-Gendebien (Ed.), ISBN: 978-953-51-1059-0, InTech.
Watanabe, T., Kanai, Y., Matsukawa, S. and Michiue, T. (2015). Specific induction of cranial placode cells from *Xenopus* ectoderm by modulating the levels of BMP, Wnt, and FGF signaling. *Genesis* **53**, 652-659.
Weinstein, D. C. and Hemmati-Brivanlou, A. (1997). Neural induction in *Xenopus laevis*: evidence for the default model. *Curr. Opin. Neurobiol.* **7**, 7-12.